

Charge-Transfer Patterns for $[\text{Ru}(\text{NH}_3)_6]^{3+/2+}$ at SAM Modified Gold Electrodes: Impact of the Permeability of a Redox Probe

Tina D. Dolidze^{a,b}, Sandra Rondinini^{*c}, Alberto Vertova^c, Mariangela Longhi^c and Dimitri E. Khoshtariya^{*a,b,d}

^aInstitute of Inorganic Chemistry and Electrochemistry, Mindeli 11, 0186, Tbilisi, Georgia

^bInstitute of Molecular Biology and Biophysics, Gotua 12, 0160 Tbilisi, Georgia

^cDepartment of Physical Chemistry and Electrochemistry, The University of Milan, Via Golgi, 19, 20133 Milan, Italy

^dDepartment of Physics, I. Javakhishvili Tbilisi State University, I. Chavchavadze Ave. 3, 0126, Tbilisi, Georgia

Abstract: Electrochemical performance of a $[\text{Ru}(\text{NH}_3)_6]^{3+/2+}$ redox couple at gold electrodes modified by alkanethiol self assembled monolayer (SAM) films of the type $[-\text{SH}-(\text{CH}_2)_n-\text{CH}_3]$ with different number of methylene units ($n = 2$ to 10) in the presence and absence of glucose additives has been studied using fast scan cyclic and steady-state voltammetry. Specific scatter of measured rate constants caused by enhanced sensitivity of this probe to minor defects of SAMs has been observed in a general agreement with the published data for thicker SAMs ($n = 9$ to 18). In addition, we have disclosed the anomalous viscosity-imposed drop of the heterogeneous rate constant for the case of Au electrodes modified by thinner n -alkanethiol SAMs ($n = 2, 4$). Taking into the account the fact of $[\text{Ru}(\text{NH}_3)_6]^{3+/2+}$ couple's capability to penetrate into the SAM interior, we ascribe the obtained results to the manifestation of the solvent-friction mechanism under the condition where the redox species presumably together with a few of solvating water molecules reside in a SAM's peripheral interior marked by much higher local viscosity (slower dielectric relaxation) compared to the electrolyte solution.

Keywords: Electrochemistry, self assembly, $\text{Ru}(\text{NH}_3)_6$, voltammetry, charge transfer, mechanisms, permeability.

1. INTRODUCTION

In depth understanding of charge transfer processes is significant from both, theoretical and practical points of view, because charge transfer is a key step in a great number of chemical and biological processes and respective knowledge is important for the construction and operation of new nanotechnological devices [1,2]. In particular, metal electrodes modified by alkanethiol self-assembled monolayer (SAM) films of different thickness and the terminal group composition have proven to be appropriate nanoscale systems for multiple technological applications and rigorous testing of charge transfer (CT) fundamentals. The persisting problem in this field is connected with the structural soundness of SAM layers and the ability of reactant species (used as redox markers – in biosensors, e.g.) either to stick to the SAM/electrolyte interface, or penetrate into the SAM interior. This point seems to be critical for functioning of electrochemical nanodevices with mobile (freely diffusing) redox markers and requires special investigations. On the grounds of previous work [1,2], hereby we strongly suggest that the insights from heterogeneous charge transfer kinetic studies should be highly informative and essentially com-

plementary to structural investigations. Hence, the modern notions on the molecular machinery of charge transfer should be extensively involved.

According to contemporary theoretical models [3-9] and recent experimental studies (performed in molecular and/or ionic liquids exploiting chemical redox markers or redox-active proteins) [10-27], heterogeneous charge transfer mechanism may display two different intrinsic mechanisms: adiabatic (solvent friction) – at short distances, and nonadiabatic (tunneling) – at long distances, as well as intermediate regime. In all cases the unimolecular rate constant (k_{et}^o) of charge transfer processes, according to the recent theoretical update, can be presented by the eq. 1 [17]:

$$k_{et}^o = \frac{(H_{if})^2}{\hbar} \frac{\rho_m}{1+g} \left(\frac{\pi^3 RT}{\lambda} \right)^{1/2} \exp\left(-\frac{\Delta G_a}{RT}\right) \quad (1)$$

where H_{if} is electronic coupling matrix element between the electrode and redox couple, ρ_m is the density of electronic states in the metal (electrode), λ is the reorganization free energy, ΔG_a is the activation free energy, R is the gas constant and T the absolute temperature. Here g is adiabaticity criterion which acts as a control parameter for the realization of either adiabatic ($g \gg 1$), or nonadiabatic ($g \ll 1$) charge transfer mechanisms and turnover between them.

The adiabaticity criterion, g , is given by the following expression [4-5,8-9,17]:

*Address correspondence to these authors at the Department of Physical Chemistry and Electrochemistry, The University of Milan, Via Golgi, 19, 20133 Milan, Italy; Tel: +39 02 503 14216; Fax: +39 02 503 14203; E-mail: sandra.rondinini@unimi.it

Institute of Molecular Biology and Biophysics, Gotua 12, 0160 Tbilisi, Georgia; Tel: +995 32 386077; Fax: +995 32 371733; E-mail: dimitri.k@joker.ge

$$g = \frac{\pi^3 RT (H_{if})^2 \rho_m}{\hbar v_{eff} \lambda} \quad (2)$$

where the effective frequency v_{eff} is related to a single or several relaxation process(es) in the vicinity of the reaction zone, that are intrinsically coupled to electron transfer. Actually, $v_{eff} \sim \eta$, where η is the medium's effective viscosity [4-9]. As one can see from eq. 2 realization and turnover between two extreme charge transfer mechanisms depends on the interplay between the values of electronic matrix element, reorganization energy and solution viscosity. Consequently, at $g \ll 1$ and $g \gg 1$ one arrives to the different expressions for the intrinsic rate constant, with the following phenomenological extensions; for the long-range (nonadiabatic) CT:

$$k_{el} \propto (H_{if})^2 \propto \exp(-\beta R_e) \quad (3)$$

where R_e is the CT distance, and β is the decay parameter normally of the order of ca. 1 \AA^{-1} , [13-17]; and for the short-range (adiabatic) CT:

$$k_{el} \propto \eta^{-\delta} \quad (4)$$

where δ is an "empirical" solvent-protein coupling parameter with values between 0 and 1, with $\delta \approx 1$ standing for full solvent-protein coupling [4-9].

Experimentally, adiabatic and nonadiabatic charge transfer mechanisms, and gradual turnover between them within the series of almost identical systems (apart from the works where limiting cases of CT mechanism have been studied separately, for different systems under different experimental conditions) were demonstrated using nanodevices made of electrode-deposited self-assembled monolayer films of variable thickness and the negatively charged model marker $[\text{Fe}(\text{CN})_6]^{3-/4-}$ [12-13], as well as for a biological molecule – protein cytochrome *c* [10, 14-17, 24]. The adiabatic mechanism for a positively charged redox couple, $[\text{Ru}(\text{NH}_3)_6]^{3+/2+}$, at bare Au electrodes, was demonstrated in our earlier work [11]. This redox couple is known to be capable to penetrate into the SAM interior, disclosing tiny defects that "invisible" for other markers (for example to $[\text{Fe}(\text{CN})_6]^{3-/4-}$, at otherwise similar conditions [13]), and show up through different kinetic patterns [28-31].

The aim of this work was to study the elementary charge-transfer mechanisms of a redox couple $[\text{Ru}(\text{NH}_3)_6]^{3+/2+}$, operating at the SAM modified gold electrodes of different thickness, searching for the mechanism turnover from the adiabatic to nonadiabatic one, under the conditions when the redox probe can permeate into the SAMs' interior. Taking into account availability of few reports for the electrochemical performance of the $[\text{Ru}(\text{NH}_3)_6]^{3+/2+}$ couple at gold electrodes modified by the long-chain SAMs ($n = 9$ to 18) [18-20] we restricted our studies to SAM modified gold electrodes with the number of methylene units $n = 2$ to 10), in order to allow for the complementary analysis together with the published data.

2. MATERIALS AND METHODS

A three electrode configuration cell with the platinum plate as an auxiliary electrode and the calomel reference electrode were used in combination with the Luggin capilla-

ry. The 1.6 mm diameter disk (sealed in a plastic cylinder) or 2 mm diameter self-made ball Au working electrodes were applied throughout. The polishing and SAM modification procedures for both types of electrodes are described elsewhere [13]. In a former case the disk electrode was cleaned with 1, 0.3 and 0.05 μm granuloses alumina from Buehler on a Buehler polishing cloth, followed by sonification in a Milli-Q water. The Au ball electrodes were cleaned by the successive rinsing in a hot and room temperature Piranha solution (3:7, 30% H_2O_2 + concentrated H_2SO_4) for 5 sec and 10 min, and the Milli-Q water, respectively. The electrodes were treated by alkanethiols, $\text{HS}-(\text{CH}_2)_n-\text{CH}_3$ ($n = 2$ to 8, Aldrich) to obtain SAM coated Au surfaces. For this purpose both kind of electrodes after cleaning procedures were rinsed by ethanol and immediately transferred into the coating solution (n-alkanethiol solution, 2×10^{-3} M in ethanol), at least for 48 h [13].

The solutions used contained 1 M NaNO_3 (Fluka) as supporting electrolyte and 1 mM $\text{Ru}(\text{NH}_3)_6\text{Cl}_3$ (Aldrich). The viscosity of solutions was varied by addition of anhydrous (+)-glucose (Fluka). Glucose concentrations of 0, 200, 402 and 602 g L^{-1} were used providing the relative viscosity values of 1.06, 1.78, 3.75, and 9.92, respectively [11-13]. Up to 6 working electrodes were used for each experiment in order to improve the statistics. The fast scan cyclic voltammetry (FSCV) and steady-state voltammetry were operated by the Amel 5000 instrument, under the control of the CorrWare software. The temperature of each experiment was 25 ± 0.5 °C. In the case of peak shaped voltammograms the rate constants of heterogeneous electron exchange were determined from the values of peak-to-peak separation (ΔE_p) according to the method of Nicholson [32], by using the numerically evaluated relationship between ΔE_p and the Ψ function, eq 5:

$$\Psi = \frac{(D_O / D_R)^{\alpha/2} (RT)^{1/2} k_{el}^o}{(\pi n F D_O \nu)^{1/2}} \quad (5)$$

where α is a transfer coefficient, R is the gas constant, T is the absolute temperature, D_O and D_R is the diffusion coefficient of the reactant's oxidized and reduced forms, respectively. In the case of non-peak shaped voltammograms kinetic data were accessed from the initial portions of steady-state curves, where the mass transport effect on the measured current was negligible [13, 21].

3. RESULTS AND DISCUSSION

Fig. (1) represents the CV curves of $[\text{Ru}(\text{NH}_3)_6]^{3+/2+}$ (recorded at 100 mV/s) for Au electrode coated by alkanethiol SAMs with a number of methylene units of $n = 2, 4$ and 8. One can see dramatic decrease of current reflecting decrease of heterogeneous rate constant, accompanying the increase of SAM thickness (the electron transfer distance) and, hence, the parameter H_{if} , in a general accordance with Eqs. 1 and 3. Fig. (2) represents semilogarithmic plots of standard rate constants for a $[\text{Ru}(\text{NH}_3)_6]^{3+/2+}$ electron exchange at SAM coated electrodes ($n = 2$ to 10) in the absence and presence of glucose, obtained in the present work, and the matching values of k_{el} for CT at the bare gold electrode obtained in our previous work [11]. The complementary results reported by Protsailo and Fawcett [18] and Kryszinski *et al.* [19-20] for thicker SAMs ($n = 9$ to 18) are also plotted for comparison. The open circles represent the rate constants in the absence

of viscous additive, and the closed circles – in the presence of 602 g/L glucose. In addition, asterisks represent data of Ref. [18], and triangles – of Refs. [19, 20].

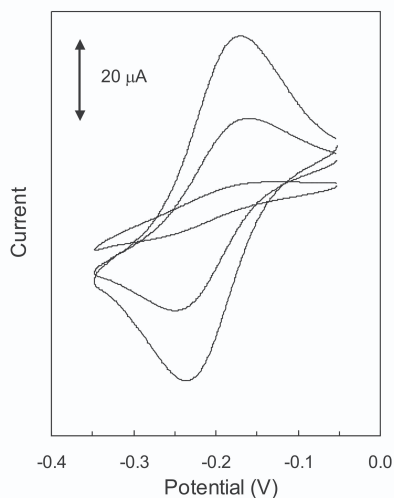


Fig. (1). CV curves of $[\text{Ru}(\text{NH}_3)_6]^{3+/2+}$ (recorded at 100 mV/s) for Au electrode ($s = 0.0314 \text{ cm}^2$) coated by alkanethiol SAMs with the number of methylene units of $n = 2, 4$ and 8 . Decrease of peak current for CV curves corresponds to the increase of methylene unit number within the SAM sequence.

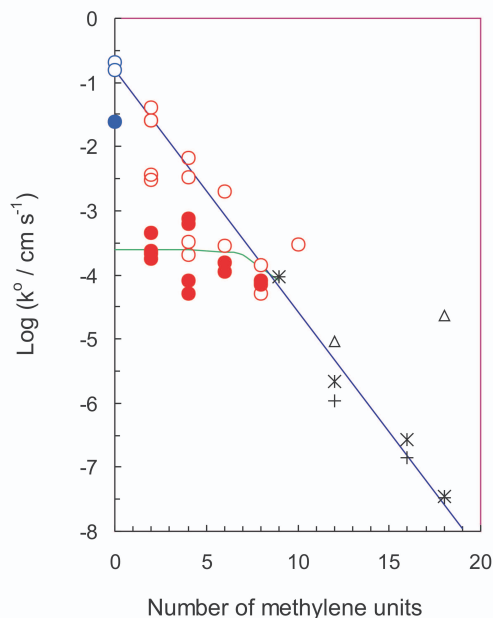


Fig. (2). Logarithm of standard rate constants for the $\text{Ru}(\text{NH}_3)_6^{3+/2+}$ electron exchange at the SAM coated electrodes with different n , obtained in the present work (circles) and by other authors [18, 20], in the absence (open circles) and presence (closed circles) of viscous additives (602 g/L glucose). Asterisks represent data of Ref. [18], and triangles – of Ref. [19, 20]. Results for bare electrode are taken from (blue open and closed circles, respectively) [11].

As one can see from Fig. (2), in the absence of glucose, the experimental points obtained both in the present work and by other authors [18-20] display remarkable scatter,

which has not been detected for the case of other, previously studied markers [13-15]. In the presence of viscous additive (glucose) the rate constants for short-chained SAMs ($n = 2, 4$) also exhibit some systematic downward deviation of experimental points. In addition rate constants for these SAMs exhibit anomalous viscosity dependence, what was not observed for other markers at otherwise similar conditions [13,15]. Fig. (3), in particular, displays semilogarithmic dependence of standard rate constants of electron exchange between $[\text{Ru}(\text{NH}_3)_6]^{3+/2+}$ and alkanethiol SAM coated Au electrodes ($n = 2, 4, 8$) on the glucose concentration. For comparison data obtained at bare gold electrode [11] are also presented. As one can see from Fig. (3), the viscosity dependence for the bare Au electrode [11] exhibits the “normal” behavior corresponding to the adiabatic charge-transfer mechanism well-documented in the previous work for different markers [11,14-15]. The curves indicated as $n = 2$ (the independent results obtained for three different electrodes), and $n = 4$ represent the viscosity-sensitive dependencies, exhibiting “anomalous” behavior. Indeed, for these cases the overall drop of rate constant varies within the broad range amounting to the 110-fold decrease in some cases (!) For the case of SAM with $n = 8$ the anomalous viscosity effect disappears (Fig. 3), whereas the over-all scatter does not (Fig. 2). It is unlikely that the specific interaction of glucose molecules with the metal electrode surface or the SAM terminal groups can be the reasons of observed anomalous viscosity effects. Indeed, Bard and coworkers [22, 23] confirmed that sugars are inert at the metal surfaces. Also, they can not interact notably with the terminal hydrophobic SAM groups due to their highly polar character.

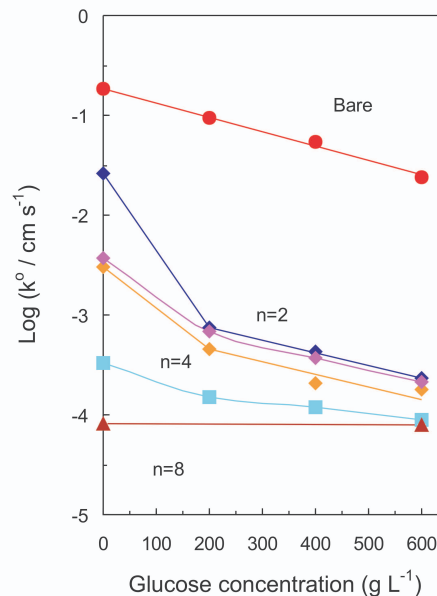


Fig. (3). Logarithm of standard rate constants for the $\text{Ru}(\text{NH}_3)_6^{3+/2+}$ electron exchange at the SAM coated electrodes with different n as a function of the glucose concentration (in g/L); rhombs: $n = 2$ (results for three independent electrodes); squares: $n = 4$; triangles: $n = 8$; The upper line (circles) represents the dependence for the bare Au electrode [11] (see text for details).

The observed experimental results can be interpreted on the basis of charge transfer theory [3-9] and the preequili-

brium model, eq. 6 [33, 34], under the conditions of a redox probe permeation through SAMs.

$$k_{EXP}^0 = k_{et}^0 K_A = k_{et}^0 \delta R_e \exp\left(\frac{-\Delta G_A}{RT}\right) \quad (6)$$

Here K_A is the statistically averaged equilibrium constant proportional to the probability of finding the reactant species at the reactive site near the electrode, δR_e is the "effective thickness" of the planar reaction zone reflecting the major portion of the space integral over the intrinsic charge transfer constant (k_{et}^0). The reactive site is usually considered to be situated at the outer Helmholtz plane (OHP) and δR_e is expected to have the value of the order of 2×10^{-9} to 10^{-8} cm [33, 34]; ΔG_A is the equilibrium free energy required to bring the reactant ion to the active site near the electrode (presumably to the OHP). For our case we will assume that $\Delta G_A \approx 0$ throughout the series.

According to most recent results, kinetically fast redox couple $[\text{Ru}(\text{NH}_3)_6]^{3+/2+}$ can detect the smallest ("invisible" for other markers) defects in the SAM, that is a manifestation of the much more sensitive nature of the $[\text{Ru}(\text{NH}_3)_6]^{3+/2+}$ couple (higher demanding conditions) to the SAM defects, compared to other markers [20, 29-32]. The latter conclusion can be justified by the recent quantum-chemical calculations of charge distribution within the complex ions, which demonstrated that in the case of hexamine metal complexes the excess charge is located on the metal core in the ion center whereas, for example, in the case of hexacyano metal complexes – on the terminal nitrogen atoms of cyano ligands [35]. Consequently, $[\text{Ru}(\text{NH}_3)_6]^{3+/2+}$ species are much more capable to penetrate into SAMs and diffuse along the SAM chains, in the presence or even absence of probable collapsed sites *versus* $[\text{Fe}(\text{CN})_6]^{3-/4-}$, e.g., reducing for some extent in randomly scattered manner the effective charge-transfer distance compared to the "ideal" case with impermeable SAMs. As a result, an average electron transfer distance for the $[\text{Ru}(\text{NH}_3)_6]^{3+/2+}$ couple would be shorter, at otherwise similar conditions, compared to the case of other "well-behaved" markers. In addition, we conjecture that in general, the SAM defects can be classified as "static" and "dynamic" ones, ascribing the former to different kind of pinholes and collapsed sites, whereas the latter – to otherwise structurally sound domains, yet with increased fluctuational mobility. We suppose that the "dynamic defects" should be of essentially cooperative nature and spread large electrode areas.

As it can be expected on the basis of general theoretical notions [3-9] and the previously obtained results [13-17, 27], penetration of redox couple into the SAM interior (that is marked by much higher local viscosity compared to the electrolyte solution) must show up in a different manner for the cases of short- and long-range CT, respectively (where two different intrinsic charge transfer mechanisms are operative), in the absence, as well as in the presence of viscous additives. Namely, for the thicker SAMs the essentially nonadiabatic behavior is expected (Eqs. 1,3), exhibiting the general dependence on the charge-transfer distance (the SAM thickness) and insensitivity to the solution (or the SAM interior) viscosity. When nonadiabatic CT mechanism is operative, penetration of the $[\text{Ru}(\text{NH}_3)_6]^{3+/2+}$ species through the SAM layers for few Ångströms, decreasing the effective charge-transfer distance in randomly scattered manner, will be ma-

nifested by the increase (in the same randomly scattered manner) of the value of rate constant compared to the "ideal" case with impermeable SAMs [13-17, 26, 27].

For the case of shortest charge-transfer distances (the thinnest SAMs), the changeover to the adiabatic (solvent-friction) regime of electron transfer is expected, exhibiting the essential viscosity dependence and pronounced plateau regions regarding the charge-transfer distance [13-17, 27]. In this case the penetration of $[\text{Ru}(\text{NH}_3)_6]^{3+/2+}$ species inside of these SAMs ($n = 2, 4$) will lead to the essential control of the charge-transfer event by the fluctuations of the SAM interior, not the solvent. SAM interior forms the quasi-crystalline environment [1] with presumably much higher local viscosity compared to the liquid electrolyte phase resulting to pronounced scatter of measured rate constants with the downward deviations (Fig. 2). Meantime, it is very probable that a few of water molecules strongly hydrogen-bonded to $[\text{Ru}(\text{NH}_3)_6]^{3+/2+}$ ions, may also diffuse through the SAMs, forming in overall complex and compactly packed fluctuating environment. The local viscosity of such a viscous "gel" still can be affected by the change of the external viscosity as it takes place in the case of biological processes involving proteins [14,15]. Interestingly, the solvent friction mechanism for the heterogeneous electron transfer rate constant of the Co(III/II) reaction of Co(II)tris(bipy) complex with the over-all 10^{10} -fold decrease of the rate constant (!) upon the viscosity variation within the similar range of degrees has been observed by Murray *et al.* [36]. In our case direct fluctuation control of CT occurring in the adiabatic regime is expected. This would lead to significant downward deviations of rate constants from alternative nonadiabatic values and their virtual insensitivity with respect of CT distance. The co-observation of high scattering could be expected due to the distribution of reactive sites situated both outside and inside the SAM interior with the participation of the $[\text{Ru}(\text{NH}_3)_6]^{3+/2+}$ marker. Another effect of the presence of glucose at the SAM/solution boundary seemingly is the increase of the marker permeability into the SAM interior. We suggest that the $[\text{Ru}(\text{NH}_3)_6]^{3+/2+}$ redox couple can be used as a detector of the SAM non-ideality for corresponding interfacial nanotechnological devices.

Note, for the case of thicker SAMs, different extent of penetration of the redox marker into the SAM interior leads to the scatter in k_{ET}^0 due to scatter of CT distance (impact *via* the parameter H_{if} , Eqs. 1,3). For the case of thinner SAMs ($n < 8$) the CT distance (and, hence the value of H_{if}) can not affect k_{et}^0 directly. In this particular case scatter may be ascribed to the variation of local relaxational properties (local viscosity) of the SAM interior caused by different configuration of defects, different extent of satellite water molecules, etc.). Analysis of kinetic data collected in Fig. (2) indicates that the average intrinsic relaxation time that controls ET in thin SAMs amounts to ca. 1 ns compared to ca. 10 ps in aqueous environments.

4. CONCLUSIONS

The alkanethiol SAMs ($n = 2$ to 8) were tested for the CT dynamics in a full adiabatic regime and marker permeability with a $[\text{Ru}(\text{NH}_3)_6]^{3+/2+}$ redox couple. High sensitivity against the nonideality (static defects and increased fluctuational mobility) of $-\text{CH}_3$ terminated SAMs has been disclosed.

However, unlike the case of thicker SAMs for which nonadiabatic mechanistic pattern is operative, penetration of a $[\text{Ru}(\text{NH}_3)_6]^{3+/2+}$ marker into the SAM interior leads to in average decrease of k_{et}^0 . This is probably due to the manifestation of the viscosity control by the SAM environment containing also a few of solvating water molecules.

The obtained results have both, fundamental and technological significance. In particular, they shed new light on the role of complex viscous environments (SAM interiors *versus* protein interiors, or ionic liquids) on the short-range CT occurring in the frictional regime. At the same time, these results help to sketch general conditions towards the selection of freely diffusing redox markers for biosensors, regarding their geometry, total charge and the charge distribution on them. In a concrete context, the $[\text{Ru}(\text{NH}_3)_6]^{3+/2+}$ redox couple can be used as a detector of the SAM non-ideality for corresponding interfacial nanotechnological devices.

ACKNOWLEDGEMENTS

D.E.K. acknowledges the Cariplo Fellowship (2002, 2005) administrated by the Landau-Volta Network (Italy). Financial support from the Ministry of Education, University and Research – The University of Milan (FIRST funds) is gratefully acknowledged.

REFERENCES

- [1] Finklea, H.O. *Self-Assembled Monolayers on Electrodes*; Encyclopedia of Analytical Chemistry Meyers, R.A. Ed.; Wiley, Chichester, **1996**, pp. 1-29.
- [2] Love, J.C.; Estroff, L.A.; Kriebel, J.K.; Nuzzo, R.G.; Whitesides, G.M. *Chem. Rev.*, **2005**, *105*, 1103-1170.
- [3] Feldberg, S.W.; Sutin, N. *Chem. Phys.*, **2006**, *324*, 216-225.
- [4] Zusman, L.D. *Chem. Phys.*, **1987**, *112*, 53-59.
- [5] Zusman, L.D. *Z. Phys. Chem.*, **1994**, *186*, 1-29.
- [6] Calef, D.F.; Wolynes, P.G. *J. Phys. Chem.*, **1983**, *87*, 3387-3400.
- [7] Hynes, J.T. *J. Phys. Chem.*, **1986**, *90*, 3701-3706.
- [8] Beratan, D.N.; Onuchic, J.N. *J. Chem. Phys.*, **1988**, *89*, 6195-6203.
- [9] Bixon, M.; Jortner, J. *Adv. Chem. Phys.*, **1999**, *106*, 35-202.
- [10] Dolidze, T.D.; Khoshtariya, D.E.; Waldeck, D.H.; Macyk, J. van Eldik, R. *J. Phys. Chem. B.*, **2003**, *107*, 7172-7179.
- [11] Khoshtariya, D.E.; Dolidze, T.D.; Vertova, A.; Longhi, M.; Rondinini, S. *Electrochem. Commun.*, **2003**, *5*, 281-245.
- [12] Khoshtariya, D.E.; Dolidze, T.D.; Krulic, D.; Fatouros, N.; Devilliers, D. *J. Phys. Chem. B.*, **1998**, *102*, 7800-7806.
- [13] Khoshtariya, D.E.; Dolidze, T.D.; Zusman, L.D.; Waldeck, D.H. *J. Phys. Chem. A.*, **2001**, *105*, 1818-1829.
- [14] Khoshtariya, D.E.; Dolidze, T.D.; Sarauli, D.; van Eldik, R. *Angew. Chem. Int. Ed.*, **2006**, *45*, 277-281.
- [15] Khoshtariya, D.E.; Dolidze, T.D.; Seyfert, S.; Sarauli, D.; Lee, G.; van Eldik, R. *Chem. Eur. J.*, **2006**, *12*, 7041-7056.
- [16] Wei, J.; Liu, H.; Khoshtariya, D.E.; Yamamoto, H.; Dick, A.; Waldeck, D.H. *Angew. Chem.*, **2002**, *114*, 4894-4897; *Angew. Chem. Int. Ed.*, **2002**, *41*, 4700-4703.
- [17] Khoshtariya, D.E.; Wei, J.; Liu, H.; Yue, H.; Waldeck, D.H. *J. Am. Chem. Soc.*, **2003**, *125*, 7704-7714.
- [18] Protsailo, L.V.; Fawcett, W.R. *Electrochim. Acta*, **2000**, *45*, 3497.
- [19] Krysinski, P.; Brzostowska-Smolka, M. *J. Electroanal. Chem.*, **1997**, *424*, 61.
- [20] Krysinski, P.; Moncelli, M.R.; Taadini-Buoninsegni, F. *Electrochim. Acta*, **2000**, *45*, 1885-1892.
- [21] Miller, C.; Cuendet, P.; Grätzel, M. *J. Phys. Chem.*, **1991**, *95*, 877-886.
- [22] Zhang, X.; Leddy, J.; Bard, A. J. *J. Am. Chem. Soc.*, **1985**, *107*, 3719-3721.
- [23] Zhang, X.; Yang, H.; Bard A. J. *J. Am. Chem. Soc.*, **1987**, *109*, 1916-1920.
- [24] Dolidze, T.D.; Rondinini, S.; Vertova, A.; Waldeck, D.H.; Khoshtariya, D.E. *Biopolymers*, **2007**, *87*, 68-73.
- [25] Dolidze, T.D.; Khoshtariya, D.E.; Illner, P.; Kulisiewicz, L.; Delgado, A.; van Eldik, R. *J. Phys. Chem. B.*, **2008**, *112*, 3085-3100.
- [26] Dolidze, T.D.; Khoshtariya, D.E.; Illner, P.; van Eldik, R. *Chem. Commun.*, **2008**, 2112-2114.
- [27] Khoshtariya, D.E.; Dolidze, T.D.; van Eldik, R. in preparation.
- [28] Diao, P.; Guo, M.; Hou, Q.; Xiang, M.; Zhang, Q. *J. Phys. Chem.*, **2006**, *110*, 20386-20391.
- [29] Calvente, J.; Lopez-peroz, G.; Ramirez, P.; Fernandez, H.; Zon, M.; Mulder, W.H.; Andreu, J. *J. Am. Chem. Soc.*, **2005**, *127*, 6476-6486.
- [30] Rondinini, S.; Vertova, A.; Pilan, L. *Electroanalysis*, **2003**, *15*, 1297-1301.
- [31] Brevnov, D.A.; Finklea, H.O. *Langmuir*, **2000**, *16*, 5973-5979.
- [32] Nicholson, R. S. *Anal. Chem.*, **1965**, *37*, 1351-1355.
- [33] Fawcett, W. R.; Foss C. A. *J. Electroanal. Chem.*, **1989**, *270*, 103-118.
- [34] Fawcett, W.R.; Hromadova, M.; Tsirlina, G.A.; Nazmutdinov, R.R. *J. Electroanal. Chem.*, **2001**, *498*, 93-104.
- [35] Hupp, J. T.; Weaver, M. J. *J. Electroanal. Chem.*, **1983**, *152*, 1-14.
- [36] Williams, E.; Crooker, J.C.; Pyati, R.; Lyons, L. J.; Murray, R. W. *J. Am. Chem. Soc.*, **1997**, *119*, 10249-10259.

Received: April 21, 2008

Revised: August 14, 2008

Accepted: September 11, 2008

© Dolidze *et al.*; Licensee Bentham Open.

This is an open access article licensed under the terms of the Creative Commons Attribution Non-Commercial License (<http://creativecommons.org/licenses/by-nc/3.0/>) which permits unrestricted, non-commercial use, distribution and reproduction in any medium, provided the work is properly cited.